A corrected version of The Farmer COSMOS2020 catalogue

J. R. Weaver, O. B. Kauffmann, O. Ilbert, H. J. McCracken, A. Moneti, S. Toft, G. Brammer, M. Shuntov, I. Davidzon, B. C. Hsieh, C. Laigle, A. Anastasiou, C. K. Jespersen, J. Vinther, P. Capak, C. M. Casey, C. J. R. McPartland, B. Milvang-Jensen, B. Mobasher, D. B. Sanders, L. Zalesky, S. Arnouts, H. Aussel, J. S. Dunlop, A. Faisst, M. Franx, L. J. Furtak, J. P. U. Fynbo, K. M. L. Gould, T. R. Greve, S. Gwyn, J. S. Kartaltepe, D. Kashino, A. M. Koekemoer, V. Kokorev, O. Le Fèvre, S. Lilly, D. Masters, G. Magdis, V. Mehta, Y. Peng, D. A. Riechers, M. Salvato, M. Sawicki, C. Scarlata, N. Scoville, R. Shirley, J. Silverman, A. Sneppen, V. Smolčić, C. Steinhardt, D. Stern, M. Tanaka, Y. Taniguchi, H. I. Teplitz, M. Vaccari, W.-H. Wang, G. Zamorani

March 5, 2023

Data Collection:	`UltraVISTA`
Release number	`4.1.1`
Data provider:	`John Weaver, Bo Milvang-Jensen, Jim Dunlop`
Date:	`March 5, 2023`

1 Abstract

COSMOS2020 (Weaver et al. 2022) consists of two catalogues named The Farmer and Classic, both containing photometry in around 40 bands and quantities such as photometric redshifts derived from SED fits. The two catalogues were released in June 2022 via ESO's Phase 3 system in the UltraVISTA collection under the label DR4.1. We have recently discovered a minor bug in The Farmer catalogue: the magnitude errors in the catalogue are moderately too small in the large error regime: for example, a reported error of 0.7 mag should have been 1.0 mag. The flux errors and all derived quantities such as photo-zs are not affected, and the Classic catalogue is not affected. The present release, with label DR4.1.1, contains a corrected version of The Farmer catalogue.

1.1 Acknowledging these data products

If you use these catalogues, please cite the following paper: "COSMOS2020: A panchromatic view of the Universe to $z \sim 10$ from two complementary catalogues", Weaver et al. (2022). You must also include the following standard acknowledgement:

"Based on observations collected at the European Southern Observatory under ESO programme ID 179.A-2005 and on data products produced by CALET and the Cambridge Astronomy Survey Unit on behalf of the UltraVISTA consortium."

If the access to the ESO Science Archive Facility services was helpful for you research, please include the following acknowledgement: "This research has made use of the services of the ESO Science Archive Facility."

You are additionally encouraged to cite the papers describing the data sets included in the catalogue (such as McCracken et al. 2012 for UltraVISTA).

2 Changes with respect to previous versions

2.1 Changes from COSMOS2015 to COSMOS2020

The previous COSMOS catalogue was COSMOS2015 (Laigle et al. 2016). It was released in Phase 3 under the label UltraVISTA DR2.1, as the catalogue was based on the UltraVISTA DR2 imaging. It was the first COSMOS catalogue to be released via Phase 3. COSMOS2015 consisted of a single catalogue. COSMOS2020 (Weaver et al. 2022) consists of two catalogues, called Classic and The Farmer (see Sect. 3.2). COSMOS2020 is based on the UltraVISTA DR4 imaging, and was first released in Phase 3 under the label UltraVISTA DR4.1 (see Sect. 2.2). The present release (DR4.1.1) fixes a minor bug in The Farmer catalogue (see Sect. 2.3).

2.2 Changes from the initial public non-Phase 3 version of COSMOS2020 to the first Phase 3 version (DR4.1)

The COSMOS2020 catalogues and supporting files were initially made publicly available on our website `https://cosmos2020.calet.org/` when the Weaver et al. paper appeared on arXiv on 28 Oct 2021 (`https://arxiv.org/abs/2110.13923`). We subsequently made an updated version, as described in Sect. 2.2.1 and 2.2.2 below. This version was released via Phase 3, and has since 24 Jun 2022 also been made available on our website, replacing the initial version.

2.2.1 Bug fixes and minor improvements

Many of the following changes were not directly due to Phase 3 requirements, but were often a result of our work preparing the Phase 3 release, and some of the bugs were discovered by ESO's Phase 3 scientist Laura Mascetti.

- Classic: negative values in the column `FLUX_RADIUS` were set to NaN
- The Farmer: corrected the column names for the four `ACS_F814W` columns (which lacked the `ACS_` part)
- The Farmer: added columns `MODEL_FLAG` and `GROUP_ID`, and removed column `VALID_SOURCE` (which was not needed after the introduction of column `MODEL_FLAG`)
- The Farmer: set all column values to NULL for sources that moved more than $0.6''$ from their detection position (these sources can be identified by the `MODEL_FLAG` column being set to 2)
- The Farmer: column `SOLUTION_MODEL` was empty, now fixed
- Classic and The Farmer: added the `ez_ssfr` column
- Classic and The Farmer: the value of the `TNULL` keywords were changed from two incorrect values to the intended value of -99
- Classic and The Farmer: the column `lp_age` was missing a unit (`TUNIT`), now fixed

- CLASSIC and THE FARMER: The catalogues contain the columns `ez_mass` (log stellar mass), `ez_sfr` (log SFR), and `ez_Lv` (log V-band luminosity). For each of these physical quantities the catalogues also contain five percentile columns, e.g. `ez_mass_p025` for the 2.5% percentile. Before the change, the values in these 3×5 percentile columns corresponded to the linear version of the quantity, while after the change they correspond to the logarithmic version

- CLASSIC and THE FARMER: the columns `lp_age`, `lp_dust`, `lp_mass_best`, `lp_SFR_best` and `lp_sSFR_best` used -99.9 to indicate NULL, which was changed to NaN

- CLASSIC: the columns `SPLASH_CH1_MAG`, `SPLASH_CH2_MAG`, `SPLASH_CH3_MAG`, `SPLASH_CH4_MAG`, `SPLASH_CH1_MAGERR`, `SPLASH_CH2_MAGERR`, `SPLASH_CH3_MAGERR` and `SPLASH_CH4_MAGERR` used -99.9 to indicate NULL, which was changed to NaN

2.2.2 Changes directly related to the Phase 3 requirements

All of the following changes relate only to the header part of the FITS files, not to the data part. These changes were made so that the data products meet the requirements defined in the ESO Science Data Products Standard document, available from the Phase 3 website[1].

- The required metadata were added to the primary headers. This includes metadata relevant to the ESO data only (here the UltraVISTA DR4 imaging in the 5 bands), such as provenance, time span, ESO programme IDs, filter names and limiting magnitudes, and metadata relevant to the catalogue as a whole, such as the footprint on the sky and the bibcode for the paper to be referenced

- For each of the almost 1200 columns in the two catalogues we wrote a description of length up to 68 characters; these descriptions are probably quite useful to the typical user. The descriptions are found in the extension 1 FITS headers (in the `TCOMM` keywords) and are listed in this document in Appendix 6.1 and 6.2

- For each column we also wrote a Unified Content Descriptor Version 1+ (UCD1+)[2]. This is a standardised vocabulary. An example could be `stat.error;phot.mag;em.opt.R` which means a statistical error on a photometric magnitude for electromagnetic radiation between 600 and 750 nm. Writing the UCDs was a substantial and complex task, and we acknowledge discussions with ESO and the IVOA Semantics group. These UCDs are found in the extension 1 header (in the `TUCD` keywords), but not given here in this document

- The extension 1 headers already contained units (in the `TUNIT` keywords), but expressed in the format/syntax of the `astropy` package (Robitaille et al. 2013; Astropy Collaboration et al. 2018). The units were changed to follow the ESO standard (see Sect. 8 of the ESO Data Interface Control Document[3]), which implements a subset of the IVOA standard[4]. The updated units are in the `TUNIT` keywords and are also listed in Appendix 6.1 and 6.2.

[1] `https://www.eso.org/sci/observing/phase3.html`
[2] `https://www.ivoa.net/documents/UCD1+/`
[3] `https://archive.eso.org/cms/tools-documentation/eso-data-interface-control.html`
[4] `https://ivoa.net/documents/VOUnits/`

Examples of changes:
`pix2` → `pix**2`
`dex(solLum)` → `log(solLum)`
`solLum-1 solMass` → `solMass/solLum`

We verified the correctness of the UCDs and units using STILTS (Taylor 2006), using votlint[5] and the VO-tools[6] (based on ucidy[7] and unity[8]), and the overall Phase 3 verification was performed by ESO. The files with the updates described in this and the previous subsections were named `R1_v2.1_p3` and are released via this ESO Phase 3 release. (See the note on filenames in Sect. 4.)

2.3 Changes from DR4.1 to DR4.1.1

We recently (early 2023) discovered that the magnitude errors in the COSMOS2020 The Farmer catalogue released in DR4.1 (filename `COSMOS2020_FARMER_R1_v2.1_p3.fits`) are moderately too small in the large error regime: for example, a reported error of 0.7 mag should have been 1.0 mag, as shown in Fig. 1. The bug was due to an editing error in the Python code.

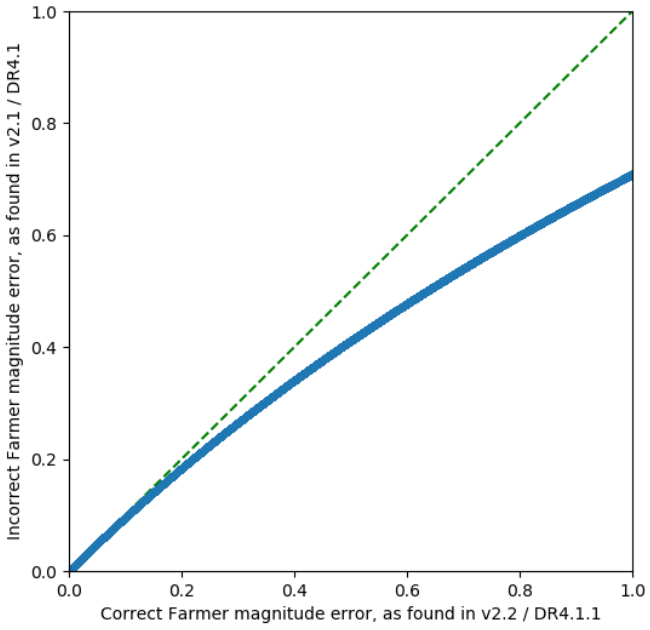

Figure 1: Comparison of magnitude errors in the two versions of The Farmer COSMOS2020 catalogue.
x-axis: Correct The Farmer magnitude error, as found in v2.2 / DR4.1.1, and
y-axis: Incorrect The Farmer magnitude error, as found in v2.1 / DR4.1.
The green dashed line marks the one-to-one relation.

[5] `http://www.star.bristol.ac.uk/~mbt/stilts/sun256/votlint.html`
[6] `http://www.star.bristol.ac.uk/~mbt/stilts/sun256/uk.ac.starlink.ttools.func.VO.html`
[7] `https://github.com/gmantele/ucidy`
[8] `https://code.nxg.name/nxg/unity`

The flux errors and all derived quantities such as photo-zs are not affected, and the CLASSIC catalogue is not affected. The present release, with label DR4.1.1 and with files named v2.2, contains a corrected version of THE FARMER catalogue (filename `COSMOS2020_FARMER_R1_v2.2_p3.fits`).

The present release does does include the CLASSIC catalogue: please obtain that from the DR4.1 release via the usual ESO interfaces. The release description document for DR4.1 can be found at `https://eso.org/rm/api/v1/public/releaseDescriptions/195` .

3 Release notes

In the following Sections, a highly condensed description of both catalogues is presented. For full details, see Weaver et al. (2022).

3.1 COSMOS2020 imaging data

The principal improvements in COSMOS2020 compared to previous COSMOS catalogues and the previous ESO Phase 3 COSMOS catalogue are the significantly deeper optical and near-infrared images from ongoing Subaru-HSC and VISTA-VIRCAM surveys. In addition, this release contains the definitive reprocessing of all Spitzer data ever taken on COSMOS. 'Legacy' or pre-existing data sets present in the previous COSMOS2015 catalogue have been reprocessed to take advantage of improved astrometry from Gaia (the only exceptions being external ancillary data such as GALEX). All images are resampled to final stacks with a $0''.15$ pixel scale. These stacks are aligned to the COSMOS tangent point, which has a right ascension and declination (J2000) of (10h00m27.92s $+02°12'03''.50$). For full details, see Weaver et al. (2022).

3.2 Photometric measurements

For the new COSMOS2020 catalogues, two independent photometric catalogues are computed using two different techniques. In both cases, the input source list is made by detecting objects on a deep $izJYHK_s$ combined `CHI-MEAN` image (defined in Appendix B of Drlica-Wagner et al. 2018) generated using `SWarp`. This image is optimised for the detection of high-redshift objects.

One catalogue is generated using the same photometric measurement methods as our previous COSMOS2015 catalogue (Laigle et al. 2016). Objects are detected with `SExtractor` (Bertin & Arnouts 1996) and for each galaxy, colours are computed using using aperture photometry performed on PSF-homogenized images (except for Spitzer/IRAC bands, where PSF-fitting with the `IRACLEAN` software (Hsieh et al. 2012) is used). This is called the "CLASSIC" catalogue.

The second photometric catalogue is created using the `The Tractor` (Lang et al. 2016) package starting from a slightly different source list derived independently with `SEP` Barbary (2016) (a `python` implementation of `SExtractor`). `The Tractor` derives parametric models from one or more images containing morphological information. An associated package, THE FARMER (Weaver et al., in prep.), generates a full multi-wavelength catalogue using `The Tractor` to perform the modelling. This approach has the advantage that `The Tractor` does not require a high-resolution image and can hence be consistently applied to ground-based data sets (and

no PSF homogenization is required). Because the models are purely parametric, `The Tractor` can provide basic shape measurements for resolved sources in addition to fluxes. Detailed comparisons of both photometric catalogues and the quality of the derived photo-z are presented in Weaver et al. (2022).

Both catalogues have their advantages and disadvantages, and the choice of which catalogue to use should be made based on the scientific application in question. Having multiple photometric redshifts for a large subset of sources can also be invaluable for validation and testing of specific measurements in COSMOS.

3.3 Photometric redshifts and physical parameters

Photometric redshifts and physical parameters are computed for both catalogues using `LePhare` (Arnouts et al. 2002; Ilbert et al. 2006) and `EAZY` (Brammer et al. 2008). Results from both packages are broadly in agreement, but once again, the choice of which package to use must be made based on the scientific application in question.

3.4 Astrometric calibration

Astrometric solutions were computed for all optical, infrared and near-infrared data using the Gaia references catalogues (DR1 or DR2; Gaia Collaboration et al. (2016, 2018)). In general, the agreement between positions of sources in each of the stacks with the external references catalogues and between sources in different bands is around 10 mas and 1 mas respectively.

4 Release Content

Table 1 lists the data products (files) in this release (DR4.1.1). Table 2 gives the correspondence between the files in DR4.1.1 and in DR4.1, for reference. Note that throughout this document, the file names are the ones we have used in our upload to the ESO Phase 3 system. Upon publication in the Phase 3 system / ESO Science Archive Facility, the files are renamed `ADP` followed by a publication timestamp. As an example, the COSMOS2015 catalogue is called `ADP.2016-12-15T11:49:34.984.fits`. ADP means Advanced Data Products. The original file name is recorded in the keyword `ORIGFILE` in the primary header. One of our data products is a tar file, containing a mix of relevant files: mask files in the form of ds9 region files, and two Python code fragments. The files in the tar file are listed in Table 3. A full description of the masks is provided in Section 4.6.

Table 1: Data products delivered with this release, i.e. DR4.1.1

Filename	Description
`COSMOS2020_FARMER_R1_v2.2_p3.fits`	The Farmer catalogue, see Section 4.4.
`COSMOS2020_FARMER_R1_v2.2_LEPHARE_PZ_p3.fits`	Redshift probability distributions, see Section 4.7
`COSMOS2020_FARMER_R1_v2.2_EAZY_CZ_p3.fits`	Redshift probability distributions, see Section 4.7
`COSMOS2020_izYJHKs_chimean-v3_COPY_p3.fits`	`CHI-MEAN` detection image
`COSMOS2020_extra_COPY_p3.tar`	Supplementary files, see Table 3

Table 2: Files in this release (DR4.1.1), and in DR4.1 for reference

File in DR4.1.1	File in DR4.1
COSMOS2020_FARMER_R1_v2.2_p3.fits	COSMOS2020_FARMER_R1_v2.1_p3.fits
COSMOS2020_FARMER_R1_v2.2_LEPHARE_PZ_p3.fits	COSMOS2020_FARMER_R1_v2.1_LEPHARE_PZ_p3.fits
COSMOS2020_FARMER_R1_v2.2_EAZY_CZ_p3.fits	COSMOS2020_FARMER_R1_v2.1_EAZY_CZ_p3.fits
COSMOS2020_izYJHKs_chimean-v3_COPY_p3.fits	COSMOS2020_izYJHKs_chimean-v3_p3.fits
COSMOS2020_extra_COPY_p3.tar	COSMOS2020_extra_p3.tar
...	COSMOS2020_CLASSIC_R1_v2.1_p3.fits
...	COSMOS2020_CLASSIC_R1_v2.1_LEPHARE_PZ_p3.fits
...	COSMOS2020_CLASSIC_R1_v2.1_EAZY_CZ_p3.fits

Table 3: Contents of the tar file

Filename	**Description**
MASK_SUPCAM_COSMOS2020.reg	Suprime-cam mask file.
MASK_HSC-stars_griz_COSMOS2020.reg	HSC mask file.
MASK_UDEEP_COSMOS2020.reg	Mask file for the Ultra-Deep regions.
MASK_UVISTA_COSMOS2020.reg	Mask file for the UltraVISTA area.
MASKS_README.txt	Description of the masks.
flags_in_catalog.png	Mask illustration (Figure 2).
eazy_zcdf_pdf.txt	Code fragment to compute photo-z PDFs from EAZY output.
COSMOS2020_prepare_apertures.txt	Code fragment to compute photometry from Classic catalogue.

4.1 Labels used for the various photometric datasets

The two COSMOS2020 catalogues contain photometry based on a number of datasets. For each of the 44 datasets we have assigned a label given in Table 4; this label is used in the column names (see the complete lists of columns names in Sections 6.1 and 6.2). Note that for most datasets we performed the photometry ourselves (Weaver et al. 2022), while for GALEX, ACS and SPLASH the photometry was crossmatched from external catalogues (see our README files in Sections 4.3 and 4.5).

4.2 The Classic catalogue

Not applicable because DR4.1.1 does not include the Classic catalogue (see DR4.1 for that).

4.3 Description of Classic catalogue columns

Not applicable because DR4.1.1 does not include the Classic catalogue (see DR4.1 for that).

4.4 The Farmer catalogue

The Farmer catalogue contains 430 columns and 964,506 rows. We provide matches with ACS, X-Ray, UV, IR, FIR and radio catalogues and also with previous COSMOS catalogues and in particular COSMOS2015. Sect. 4.5 provides the README file distributed with the catalogue

Table 4: The photometric datasets

Label	Description	$\lambda_{\rm central}$ [Å]	width[Å]
GALEX_FUV	GALEX FUV	1526	224
GALEX_NUV	GALEX NUV	2307	791
CFHT_u	CFHT/MegaCam u	3709	518
CFHT_ustar	CFHT/MegaCam u*	3858	598
ACS_F814W	HST/ACS F814W	8333	2511
HSC_g	Subaru/HSC HSC-SSP PDR2 g	4847	1383
HSC_r	Subaru/HSC HSC-SSP PDR2 r	6219	1547
HSC_i	Subaru/HSC HSC-SSP PDR2 i	7699	1471
HSC_z	Subaru/HSC HSC-SSP PDR2 z	8894	766
HSC_y	Subaru/HSC HSC-SSP PDR2 y	9761	786
SC_B	Subaru/SuprimeCam B	4488	892
SC_gp	Subaru/SuprimeCam g+	4804	1265
SC_V	Subaru/SuprimeCam V	5487	954
SC_rp	Subaru/SuprimeCam r+	6305	1376
SC_ip	Subaru/SuprimeCam i+	7693	1497
SC_zp	Subaru/SuprimeCam z+	8978	847
SC_zpp	Subaru/SuprimeCam z++	9063	1335
SC_IB427	Subaru/SuprimeCam IB427	4266	207
SC_IB464	Subaru/SuprimeCam IB464	4635	218
SC_IA484	Subaru/SuprimeCam IA484	4851	229
SC_IB505	Subaru/SuprimeCam IB505	5064	231
SC_IA527	Subaru/SuprimeCam IA527	5261	243
SC_IB574	Subaru/SuprimeCam IB574	5766	273
SC_IA624	Subaru/SuprimeCam IA624	6232	300
SC_IA679	Subaru/SuprimeCam IA679	6780	336
SC_IB709	Subaru/SuprimeCam IB709	7073	316
SC_IA738	Subaru/SuprimeCam IA738	7361	324
SC_IA767	Subaru/SuprimeCam IA767	7694	365
SC_IB827	Subaru/SuprimeCam IB827	8243	343
SC_NB711	Subaru/SuprimeCam NB711	7121	72
SC_NB816	Subaru/SuprimeCam NB816	8150	120
UVISTA_Y	VISTA/VIRCAM UltraVISTA DR4 Y	10216	923
UVISTA_J	VISTA/VIRCAM UltraVISTA DR4 J	12525	1718
UVISTA_H	VISTA/VIRCAM UltraVISTA DR4 H	16466	2905
UVISTA_Ks	VISTA/VIRCAM UltraVISTA DR4 Ks	21557	3074
UVISTA_NB118	VISTA/VIRCAM UltraVISTA DR4 NB118	11909	112
IRAC_CH1	Spitzer/IRAC ch1	35686	7443
IRAC_CH2	Spitzer/IRAC ch2	45067	10119
IRAC_CH3	Spitzer/IRAC ch3	57788	14082
IRAC_CH4	Spitzer/IRAC ch4	79958	28796
SPLASH_CH1	Spitzer/IRAC SPLASH ch1	35686	7443
SPLASH_CH2	Spitzer/IRAC SPLASH ch2	45067	10119
SPLASH_CH3	Spitzer/IRAC SPLASH ch3	57788	14082
SPLASH_CH4	Spitzer/IRAC SPLASH ch4	79958	28796

Note: see also Table 1 in Weaver et al. (2022).

describing each column. Additionally, in Sect. 6.2 we list of all the 430 columns together with their number, name, and description.

4.5 Description of The Farmer catalogue columns

```
The FARMER COSMOS2020 photometric catalog

We present here the catalog containing the photometry detected with SEP on a izYJHKs CHI-MEAN image
and extracted with The Tractor for about 1,000,000 sources in the COSMOS field within the areas of
UltraVISTA and outside the HSC bright star haloes. Suitable models are determined with izYJHKs imaging
for all detected sources, convolved with the PSF of a given band and optimised to measure flux
which is treated as a free parameter. Model parameters (radius, shape, etc.) are available upon request.
The full description of this catalog is in Weaver et al., 2022a (ApJS 258 11)

Updated 02/2022
contact: john.weaver.astro@gmail.com

#########################################################
Identification
#########################################################

Identifier
#   name = 'ID'

Right Ascension and Declination
#   name = 'ALPHA_J2000'; unit = 'deg'
#   name = 'DELTA_J2000'; unit = 'deg'

Coordinates above are based on model centroids, or SEP when models not available

Position, as determined by model centroid
#   name = 'X_MODEL'; unit = 'pixel'
#   name = 'Y_MODEL'; unit = 'pixel'
#   name = 'ERRX_MODEL'; unit = 'pixel'
#   name = 'ERRY_MODEL'; unit = 'pixel'

Position, as determined by SEP at detection, in J2000
#   name = 'ALPHA_DETECTION'; unit = 'deg'
#   name = 'DEC_DETECTION'; unit = 'deg'

Farmer model information
#   name = 'FARMER_ID'       Farmer internal source identifier ({brick}_{source})
#   name = 'GROUP_ID'        Farmer group identifier; unique within a brick
#   name = 'N_GROUP'         Farmer group occupation number
#   name = 'MODEL_FLAG'      (0: OK, 1: failed to converge, 2: drifted >0.6" from detection)
#   name = 'SOLUTION_MODEL'  The Tractor model type selected by The Farmer

Model shape information may be provided in a future release.

#########################################################
Flags
#########################################################

Flag for the bright stars and edges of the HSC images
#   name = 'FLAG_HSC'      (0:clean, 1:masked)

Flag for the bright stars and edges of the Suprime-Cam images
#   name = 'FLAG_SUPCAM'   (0:clean, 1:masked)

Flag for the UltraVISTA region
#   name = 'FLAG_UVISTA'   (0:inside, 1:outside)

Flag for the UltraVISTA ultra-deep regions
```

```
#   name = 'FLAG_UDEEP'    (0:ultra-deep, 1:deep)

Flag for the combination of FLAG_UVISTA, FLAG_HSC and FLAG_SUPCAM
#   name = 'FLAG_COMBINED' (0:clean and inside UVISTA)

#########################################################
Galactic extinction at the object position
#########################################################

E(B-V) values from Schlegel, Finkbeiner & Davis (1998) dust map
By default, a scaling of 0.86 is applied to the map values
to reflect the recalibration by Schlafly & Finkbeiner (2011)

#   name = 'EBV_MW'; unit = 'mag'

#########################################################
Photometry
#########################################################

No data convention
flux, fluxerr, mag, magerr = NaN

Negative flux convention
mag, magerr = NaN

NOTE: The photometry are not corrected for Milky Way extinction.
NOTE: The photometry are not corrected for photometric offsets derived by LePhare or EAZY
NOTE: The photometry errors are not corrected for the correlated noise in the images.

#########################################################

List of bands
CFHT/MegaCam (CLAUDS): ustar, u
Subaru/HSC: g, r, i, z, y
VISTA/VIRCAM (UltraVISTA DR4): Y, J, H, Ks, NB118
Subaru/Suprime-Cam: IB427, IB464, IA484, IB505, IA527, IB574, IA624, IA679, IB709, IA738,
                    IA767, IB827, NB711, NB816
Sptizer/IRAC (Cosmic DAWN Survey): IRAC_CH1, IRAC_CH2, IRAC_CH3, IRAC_CH4

NOTE: SuprimeCam Broad bands are not measured with Farmer

Total model fluxes, flux errors, magnitudes and magnitude errors
#   name = '###_FLUX';    unit = 'uJy'
#   name = '###_FLUXERR'; unit = 'uJy'
#   name = '###_MAG';     unit = 'mag'
#   name = '###_MAGERR'; unit = 'mag'

NOTE: aperture corrections should not be applied


#   name = '###_CHISQ'  Reduced Chi2 goodness of fit statistic for source profile model
#   name = '###_DRIFT'  Distance travelled from ALPHA/DELTA_J2000 (i.e. model centroid)
#   name = '###_VALID'  Set to False where FLUX or FLUXERR not trustworthy

#   name = 'VALID_SOURCE'    Set to False when photometry failed
#   name = 'SOLUTION_MODEL'  The Tractor model type selected by The Farmer

#####################################################
Ancillary photometry

NOTE: All are matched within 0.6" radius
#####################################################

GALEX photometry (Zamojski et al. 2007) from the Capak et al. 2007 catalog
```

```
Matched identifier
#   name = 'ID_GALEX'

List of bands
  GALEX_NUV, GALEX_FUV

#   name = '###_FLUX';    unit = 'uJy'
#   name = '###_FLUXERR'; unit = 'uJy'
#   name = '###_MAG';    unit = 'mag'
#   name = '###_MAGERR'; unit = 'mag'

#####################################################

SPLASH photometry from the COSMOS2015 catalog (Laigle et al. 2016)

Matched identifier
#   name = 'ID_COSMOS2015'

List of bands
  SPLASH_CH1, SPLASH_CH2, SPLASH_CH3, SPLASH_CH4

#   name = '###_FLUX';    unit = 'uJy'
#   name = '###_FLUXERR'; unit = 'uJy'
#   name = '###_MAG';    unit = 'mag'
#   name = '###_MAGERR'; unit = 'mag'

#####################################################

HST/ACS catalog (Leauthaud et al. 2007)
selection: CLEAN == 1

Matched identifier
#   name = 'ID_ACS'

ACS photometry
#   name = 'ACS_F814W_FLUX';    unit = 'uJy'
#   name = 'ACS_F814W_FLUXERR'; unit = 'uJy'
#   name = 'ACS_F814W_MAG';    unit = 'mag'
#   name = 'ACS_F814W_MAGERR'; unit = 'mag'

ACS morphology
#   name = 'ACS_A_WORLD'; unit = 'deg'
#   name = 'ACS_B_WORLD'; unit = 'deg'
#   name = 'ACS_THETA_WORLD'; unit = 'deg'
#   name = 'ACS_FWHM_WORLD'; unit = 'deg'
#   name = 'ACS_MU_MAX'; unit = 'mag'
#   name = 'ACS_MU_CLASS'

#####################################################

Chandra COSMOS-Legacy Survey (Civano et al. 2016, Marchesi et al. 2016)

Matched identifier
#   name = 'ID_CHANDRA'

#####################################################

Corresponding Classic 2020 source

Matched identifier
#   name = 'ID_CLASSIC'

#####################################################
Le Phare photo-z and physical parameters
#####################################################
```

```
# NOTE: MW correction derived from Schlafly&Finkbeiner+2011 values assuming Allen+1976 reddening

Photometric Redshift
Derived using a method similar to Ilbert et al. (2009, 2013)
#  name = 'lp_zBEST'

   z = zPDF  if galaxy  (median of the likelihood distribution)
   z = NaN   if star, Xray source based on Chandra (Civiano program), or masked area (FLAG_HSC|FLAG_SC|FLAG_UVISTA)

Star/Galaxy Separation
See paper for details
#  name = 'lp_type'

    type=0   if galaxy
    type=1   if star (mainly 3.6 micron, and half-light radius in HSC and HST)
    type=2   if Xray source
    type=-9  if failure in the fit (most of these objects have less than 1 band)



Best fit obtained with the galaxy templates
#  name = 'lp_zPDF'           photo-z (defined as the median of the likelihood) measured using the galaxy templates
#  name = 'lp_zPDF_l68'       lower limit, 68% confidence level
#  name = 'lp_zPDF_u68'       upper limit, 68% confidence level

#  name = 'lp_zMinChi2'       photo-z (defined as the minimum of the chi2) measured using the galaxy templates
#  name = 'lp_chi2_best'      reduced chi2 (-99 if less than 3 filters) for zMinChi2

#  name = 'lp_zp_2'           second photo-z solution if a second peak is detected with P>5% in the PDF
#  name = 'lp_chi2_2'         reduced chi2 for the second photo-z solution

#  name = 'lp_NbFilt'         Number of filters used in the fit

NOTE: Every source has a redshift, regardless of the type or if it is in a masked area or not

##########################################################

Best fit obtained with the AGN templates
#  name = 'lp_zq'             photoz for the AGN library.
#  name = 'lp_chiq'           reduced chi2
#  name = 'lp_modq'           best fit template

NOTE: This value is only informative: no correction for variability is applied.

##########################################################

Best fit obtained with the STAR templates

#  name = 'lp_mods'           model for the star library
#  name = 'lp_chis'           reduced chi2

##########################################################

Corresponding mask flag if masked by FLAG_UVISTA | FLAG_HSC | FLAG_SC

#  name = 'lp_mask'

##########################################################

Physical Properties
Derived from the BC03 best-fit templates at zPDF
(Chabrier IMF; cosmo:70,0.3,0.7; BC03 tau+delayed models described in Ilbert et al. 2015).
NOTE: A value is computed for all sources, even the one in masked area or classified as star

Best fit BC03 model at zPDF
```

```
#  name = 'lp_model'                    best-fit model index
#  name = 'lp_age'                      age of best-fit template in years
#  name = 'lp_dust'                     best-fit color excess E(B-V)
#  name = 'lp_Attenuation'              best-fit dust law index

Absolute rest-frame AB magnitudes
#  name = 'lp_MFUV'                  FUV galex
#  name = 'lp_MNUV'                  NUV galex
#  name = 'lp_MU'                    U  cfht new
#  name = 'lp_MG'                    g  Subaru HSC
#  name = 'lp_MR'                    r  Subaru HSC
#  name = 'lp_MI'                    i  Subaru HSC
#  name = 'lp_MZ'                    z  Subaru HSC
#  name = 'lp_MY'                    Y VISTA
#  name = 'lp_MJ'                    J VISTA
#  name = 'lp_MH'                    H VISTA
#  name = 'lp_MK'                    Ks VISTA

Galaxy Stellar Mass
#  name = 'lp_mass_med'           log Stellar mass from BC03 best-fit template. median of the PDF
#  name = 'lp_mass_med_min68'     lower limit, 68% confidence level
#  name = 'lp_mass_med_max68'     upper limit, 68% confidence level
#  name = 'lp_mass_best'          log Stellar mass from BC03 best-fit template. Taken at the minimum chi2

SFR and sSFR
#  name = 'lp_SFR_med'            log SFR from BC03 best-fit template. median of the PDF
#  name = 'lp_SFR_med_min68'      lower limit, 68% confidence level
#  name = 'lp_SFR_med_max68'      upper limit, 68% confidence level
#  name = 'lp_SFR_best'           log SFR from BC03 best-fit template. Taken at the minimum chi2

#  name = 'lp_sSFR_med'            log sSFR from BC03 best-fit template. median of the PDF
#  name = 'lp_sSFR_med_min68'      lower limit, 68% confidence level
#  name = 'lp_sSFR_med_max68'      upper limit, 68% confidence level
#  name = 'lp_sSFR_best'           log sSFR from BC03 best-fit template. Taken at the minimum chi2

NOTE: SFR and sSFR is computed without IR, large uncertainties with such methods

####################################################
EAZY photo-z and physical parameters
####################################################
NOTE: EAZY uses one value of Galactic extinction for all sources: E(B-V) = 0.017

Photometric redshift
Derived using the latest development version of eazy-py. See paper for details.
#  name = 'ez_z_phot'              maximum a-posteriori photometric redshift
#  name = 'ez_z_phot_chi2'         chi2 at z_phot, with z-prior
#  name = 'ez_z_phot_risk'         risk parameter from Tanaka+2018; R(ez_z_phot)
#  name = 'ez_z_min_risk'          redshift where R(z) is minimised
#  name = 'ez_min_risk'         R(ez_z_min_risk)
#  name = 'ez_z_raw_chi2'                redshift where chi2 is minimised, without priors
#  name = 'ez_raw_chi2'         chi2 at ez_z_raw_chi2

Redshift probability distribution percentiles
#  name = 'ez_z###'                     025, 160, 500, 840, 975 corresponds to 2.5%, 16%, 50%, 84%, 97.5%

Fitting parameters
#  name = 'ez_nusefilt'         number of filters used for photo-z (i.e., not masked as missing data)
#  name = 'ez_lc_min'           minimum effective wavelength of valid filters, Angstrom
#  name = 'ez_lc_max'           maximum effective wavelength of valid filters, Angstrom

Best-fit stellar templates
#  name = 'ez_star_min_chi2'    chi2 of best stellar template fit (BT-SETTL models); assumes 8% systematic uncertainty
#  name = 'ez_star_teff'        effective temperature of the stellar template; unit = 'K'

####################################################
```

```
Physical Properties
Derived from the FSPS best-fit templates (Chabrier IMF; cosmo:69.4,0.287,0.713 - WMAP9).
Dust is applied by hand using the Kriek+Conroy attenuation curve (delta=0)
Total energy absorbed by this dust screen (energy_abs) is computed, and a corresponding far-IR component is added to
the SED using the templates from Magdis+2012.

Absolute rest-frame AB magnitudes
The templates are used to perform a weighted interpolation of the rest-frame filter by refitting the templates
at ez_z_phot but with the uncertainties weighted to favour observed-frame measurements closest to the desired rest-frame band.
#  name = 'ez_restU'                    rest-frame U-band flux (units of catalog fluxes, uJy)
#  name = 'ez_restU_err'                rest-frame U-band flux uncertainty (units of catalog fluxes, uJy)
#  name = 'ez_restB'                    rest-frame B-band flux (units of catalog fluxes, uJy)
#  name = 'ez_restB_err'                rest-frame B-band flux uncertainty (units of catalog fluxes, uJy)
#  name = 'ez_restV'                    rest-frame V-band flux (units of catalog fluxes, uJy)
#  name = 'ez_restV_err'                rest-frame V-band flux uncertainty (units of catalog fluxes, uJy)
#  name = 'ez_restJ'                    rest-frame J-band flux (units of catalog fluxes, uJy)
#  name = 'ez_restJ_err'                rest-frame J-band flux uncertainty (units of catalog fluxes, uJy)

Miscellaneous properties
#  name = 'ez_dL'                       luminosity distance at z_phot; unit = 'Mpc'
#  name = 'ez_mass'                     log(mass in Msun)
#  name = 'ez_sfr'                      log(sfr in Msun/yr)
#  name = 'ez_ssfr'                     log(ssfr in 1/yr)
#  name = 'ez_Lv'                       log(V-band luminosity in Lsun)
#  name = 'ez_LIR'                      total 8-1000um luminosity in Lsun)
#  name = 'ez_energy_abs'               implied absorbed energy associated with Av; unit = 'Lsun'
#  name = 'ez_Lu'                       luminosity in U-band; unit = 'Lsun'
#  name = 'ez_Lj'                       luminosity in J-band; unit = 'Lsun'
#  name = 'ez_L1400'                    luminosity tophat filter at 1400 A; unit = 'Lsun'
#  name = 'ez_L2800'                    luminosity tophat filter at 2800 A; unit = 'Lsun'
#  name = 'ez_LHa'                      Ha line luminosity (reddened), unit = 'Lsun'
#  name = 'ez_LOIII'                    OIII line luminosity (reddened), unit = 'Lsun'
#  name = 'ez_LHb'                      Hb line luminosity (reddened), unit = 'Lsun'
#  name = 'ez_LOII'                     OII line luminosity (reddened), unit = 'Lsun'
#  name = 'ez_MLv'                      mass-to-light ratio in V-band; unit = 'Msun/Lsun'
#  name = 'ez_Av'                       extinction in V-band; unit = 'Mag'
#  name = 'ez_lwAgeV'                   light-weighted age in the V-band; unit = 'Gyr'

Property percentiles
Five percentiles (025, 160, 500, 840, 975 corresponds to 2.5%, 16%, 50%, 84%, 97.5%) are computed for the following properties:
ez_mass, ez_sfr, ez_ssfr, ez_Lv, ez_LIR, ez_energy_abs, ez_Lu, ez_Lj, ez_L1400, ez_L2800, ez_L2800, ez_Ha, ez_OIII,
ez_Hb, ez_OII. All are stated in the same scaling and units as their non-percentile columns.
#  name = 'ez_XXXX_p###'
```

4.6 Masks

In the COSMOS2020 catalogues, binary flags are used to identify different regions. Four areas are indicated: the region covered by the UltraVISTA survey (`FLAG_UVISTA`), the region covered by 'ultra-deep' stripes within the UltraVISTA survey (`FLAG_UDEEP`), the area covered by bright stars in the HSC survey (`FLAG_HSC`) and the area covered by bright stars in the legacy Suprime-cam data (`FLAG_SUPCAM`). Throughout, the same convention is used: for objects with `flag == 1` the object is within the masked region and should not be used. Objects with `flag == 0` are outside the masked region. These different masks are summarized in Table 5 and graphically in Figure 2. Also listed are the `ds9`[9] region files which are being made available with this release.

[9] `sites.google.com/cfa.harvard.edu/saoimageds9/home`

Table 5: A summary of the flags provided in the catalogue together with their associated region files.

Mask name	Area (deg^2)	Region file
FLAG_HSC	2.75	MASK_HSC-stars_griz.reg
FLAG_UVISTA	1.792	MASK_UVISTA.reg
FLAG_UDEEP	1.054	MASK_UDEEP.reg
FLAG_SUPCAM	1.918	MASK_SUPCAM.reg
FLAG_COMBINED	1.27	(all of the above except UDEEP)

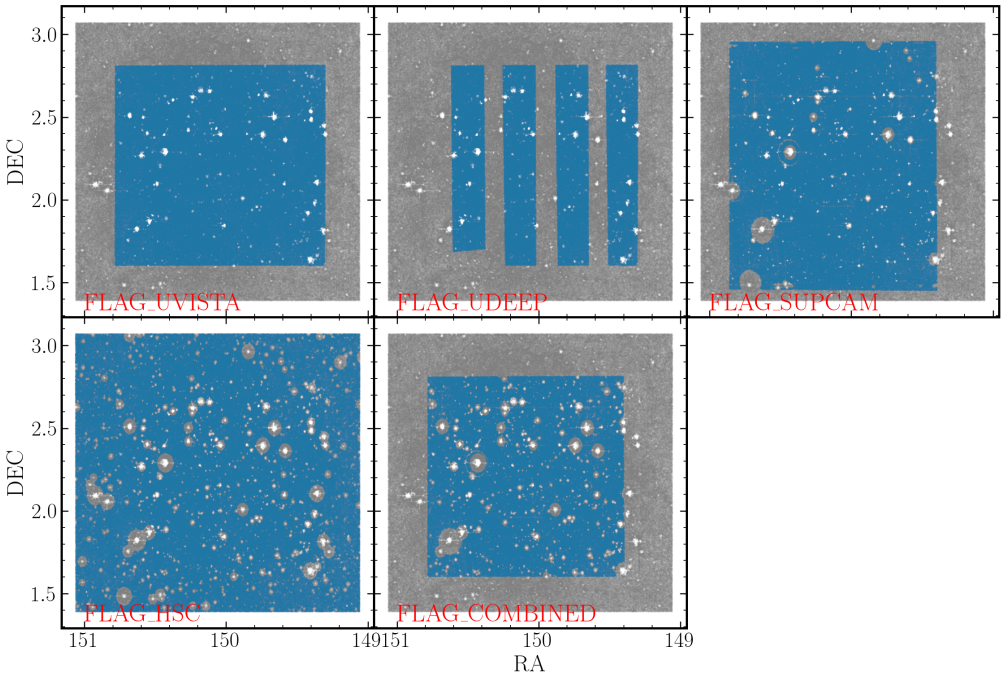

Figure 2: An illustration of the areas covered by each of the five different mask types present in the catalogue. Blue regions show the zones covered by the masks.

4.7 Redshift probability distributions

For each source, in both catalogues, we provide the redshift probability distributions or $p(z)$. These are stored as fits files.

The $p(z)$ results from `LePhare` are recorded as the likelihood at a given redshift spanning a baseline from $z = 0$ to 10 sampling in 1001 points of equal-z.

Slightly differently, the $p(z)$ results from `EAZY` are stored instead as 50 samplings of the cumulative redshift probability distribution or $cdf(z)$, equally spaced according to multiples of the standard deviation of a Gaussian distribution. As such, the $p(z)$ can be easily reconstructed from the relatively more compact $cdf(z)$ data without a significant loss of precision. Alternatively, users may find it advantageous to simply assess the probability of a source being in a certain redshift range by taking the difference in the $cdf(z)$ at two z points, equivalent to integrating the $p(z)$ but with much less computational effort. A script is provided to help users access and use this format.

4.8 Other products

Before photometric redshift measurements are made from photometric data, a series of corrections are applied to each object. These include correction of Milky Way extinction based on the value of $E(B - V)$ derived from dust maps and the application of a series of aperture offsets to bring individual colours to total photometry. At the release website, Classic catalogue, we provide a `Python` program to compute this offset.

5 Acknowledgements

A full list of acknowledgements for the data sources used in this catalogue, together with their associated bibliographic references, can be found in Weaver et al. (2022).

6 Appendices

6.1 Complete list of Classic catalogue columns

Not applicable because DR4.1.1 does not include the Classic catalogue (see DR4.1 for that).

6.2 Complete list of The Farmer catalogue columns

The following is a list of number, name, description and unit for all the columns in The Farmer.

No.	Column name	Column description	Column unit
1	ID	ID (specifically ID_FARMER, as this is the Farmer catalogue)	
2	ALPHA_J2000	Right ascension (J2000) of model, or of SEP when model is not avail.	deg
3	DELTA_J2000	Declination (J2000) of model, or of SEP when model is not available	deg
4	X_MODEL	Object model position along X, with the scale being 0.15"/px	pix

5	Y_MODEL	Object model position along Y, with the scale being 0.15"/px	pix
6	ERRX_MODEL	Uncertainty on object model position along X	pix
7	ERRY_MODEL	Uncertainty on object model position along Y	pix
8	ALPHA_DETECTION	Right ascension (J2000) of object as determined by SEP at detection	deg
9	DELTA_DETECTION	Declination (J2000) of object as determined by SEP at detection	deg
10	FARMER_ID	Farmer internal source identifier ({brick}_{source})	
11	GROUP_ID	Farmer group identifier; unique within a brick	
12	N_GROUP	Farmer group occupation number	
13	MODEL_FLAG	Flag (0: OK, 1: failed to converge, 2: drifted >0.6" from detection)	
14	SOLUTION_MODEL	The Tractor model type selected by The Farmer	
15	FLAG_HSC	Flag indicating quality of HSC imaging (0:clean, 1:masked)	
16	FLAG_SUPCAM	Flag indicating quality of Suprime-Cam imaging (0:clean, 1:masked)	
17	FLAG_UDEEP	Flag for the UltraVISTA ultra-deep regions (0:ultra-deep, 1:deep)	
18	FLAG_UVISTA	Flag for the UltraVISTA region (0:inside, 1:outside)	
19	FLAG_COMBINED	Comb. FLAG_UVISTA, FLAG_HSC, FLAG_SUPCAM (0:clean and inside UVISTA)	
20	EBV_MW	Galactic reddening E(B-V) (Schlegel+1998, Schlafly&Finkbeiner 2011)	
21	CFHT_u_FLUX	CFHT_u flux density	uJy
22	CFHT_u_FLUXERR	CFHT_u flux density error	uJy
23	CFHT_u_MAG	CFHT_u AB magnitude	mag
24	CFHT_u_MAGERR	CFHT_u AB magnitude error	mag
25	CFHT_u_CHISQ	CFHT_u reduced Chi2 goodness of fit stat for source prof model	
26	CFHT_u_DRIFT	CFHT_u distance travelled from RA,Dec model centroid	arcsec
27	CFHT_u_VALID	CFHT_u flag=False if FLUX/MAG or its error is not trustworthy	
28	CFHT_ustar_FLUX	CFHT_ustar flux density	uJy
29	CFHT_ustar_FLUXERR	CFHT_ustar flux density error	uJy
30	CFHT_ustar_MAG	CFHT_ustar AB magnitude	mag
31	CFHT_ustar_MAGERR	CFHT_ustar AB magnitude error	mag
32	CFHT_ustar_CHISQ	CFHT_ustar reduced Chi2 goodness of fit stat for source prof model	
33	CFHT_ustar_DRIFT	CFHT_ustar distance travelled from RA,Dec model centroid	arcsec
34	CFHT_ustar_VALID	CFHT_ustar flag=False if FLUX/MAG or its error is not trustworthy	
35	HSC_g_FLUX	HSC_g flux density	uJy
36	HSC_g_FLUXERR	HSC_g flux density error	uJy
37	HSC_g_MAG	HSC_g AB magnitude	mag
38	HSC_g_MAGERR	HSC_g AB magnitude error	mag
39	HSC_g_CHISQ	HSC_g reduced Chi2 goodness of fit stat for source prof model	
40	HSC_g_DRIFT	HSC_g distance travelled from RA,Dec model centroid	arcsec
41	HSC_g_VALID	HSC_g flag=False if FLUX/MAG or its error is not trustworthy	
42	HSC_r_FLUX	HSC_r flux density	uJy
43	HSC_r_FLUXERR	HSC_r flux density error	uJy
44	HSC_r_MAG	HSC_r AB magnitude	mag
45	HSC_r_MAGERR	HSC_r AB magnitude error	mag
46	HSC_r_CHISQ	HSC_r reduced Chi2 goodness of fit stat for source prof model	
47	HSC_r_DRIFT	HSC_r distance travelled from RA,Dec model centroid	arcsec
48	HSC_r_VALID	HSC_r flag=False if FLUX/MAG or its error is not trustworthy	
49	HSC_i_FLUX	HSC_i flux density	uJy
50	HSC_i_FLUXERR	HSC_i flux density error	uJy
51	HSC_i_MAG	HSC_i AB magnitude	mag
52	HSC_i_MAGERR	HSC_i AB magnitude error	mag
53	HSC_i_CHISQ	HSC_i reduced Chi2 goodness of fit stat for source prof model	
54	HSC_i_DRIFT	HSC_i distance travelled from RA,Dec model centroid	arcsec
55	HSC_i_VALID	HSC_i flag=False if FLUX/MAG or its error is not trustworthy	
56	HSC_z_FLUX	HSC_z flux density	uJy
57	HSC_z_FLUXERR	HSC_z flux density error	uJy
58	HSC_z_MAG	HSC_z AB magnitude	mag
59	HSC_z_MAGERR	HSC_z AB magnitude error	mag
60	HSC_z_CHISQ	HSC_z reduced Chi2 goodness of fit stat for source prof model	
61	HSC_z_DRIFT	HSC_z distance travelled from RA,Dec model centroid	arcsec
62	HSC_z_VALID	HSC_z flag=False if FLUX/MAG or its error is not trustworthy	
63	HSC_y_FLUX	HSC_y flux density	uJy
64	HSC_y_FLUXERR	HSC_y flux density error	uJy
65	HSC_y_MAG	HSC_y AB magnitude	mag
66	HSC_y_MAGERR	HSC_y AB magnitude error	mag
67	HSC_y_CHISQ	HSC_y reduced Chi2 goodness of fit stat for source prof model	
68	HSC_y_DRIFT	HSC_y distance travelled from RA,Dec model centroid	arcsec
69	HSC_y_VALID	HSC_y flag=False if FLUX/MAG or its error is not trustworthy	

70	UVISTA_Y_FLUX	UVISTA_Y flux density	uJy
71	UVISTA_Y_FLUXERR	UVISTA_Y flux density error	uJy
72	UVISTA_Y_MAG	UVISTA_Y AB magnitude	mag
73	UVISTA_Y_MAGERR	UVISTA_Y AB magnitude error	mag
74	UVISTA_Y_CHISQ	UVISTA_Y reduced Chi2 goodness of fit stat for source prof model	
75	UVISTA_Y_DRIFT	UVISTA_Y distance travelled from RA,Dec model centroid	arcsec
76	UVISTA_Y_VALID	UVISTA_Y flag=False if FLUX/MAG or its error is not trustworthy	
77	UVISTA_J_FLUX	UVISTA_J flux density	uJy
78	UVISTA_J_FLUXERR	UVISTA_J flux density error	uJy
79	UVISTA_J_MAG	UVISTA_J AB magnitude	mag
80	UVISTA_J_MAGERR	UVISTA_J AB magnitude error	mag
81	UVISTA_J_CHISQ	UVISTA_J reduced Chi2 goodness of fit stat for source prof model	
82	UVISTA_J_DRIFT	UVISTA_J distance travelled from RA,Dec model centroid	arcsec
83	UVISTA_J_VALID	UVISTA_J flag=False if FLUX/MAG or its error is not trustworthy	
84	UVISTA_H_FLUX	UVISTA_H flux density	uJy
85	UVISTA_H_FLUXERR	UVISTA_H flux density error	uJy
86	UVISTA_H_MAG	UVISTA_H AB magnitude	mag
87	UVISTA_H_MAGERR	UVISTA_H AB magnitude error	mag
88	UVISTA_H_CHISQ	UVISTA_H reduced Chi2 goodness of fit stat for source prof model	
89	UVISTA_H_DRIFT	UVISTA_H distance travelled from RA,Dec model centroid	arcsec
90	UVISTA_H_VALID	UVISTA_H flag=False if FLUX/MAG or its error is not trustworthy	
91	UVISTA_Ks_FLUX	UVISTA_Ks flux density	uJy
92	UVISTA_Ks_FLUXERR	UVISTA_Ks flux density error	uJy
93	UVISTA_Ks_MAG	UVISTA_Ks AB magnitude	mag
94	UVISTA_Ks_MAGERR	UVISTA_Ks AB magnitude error	mag
95	UVISTA_Ks_CHISQ	UVISTA_Ks reduced Chi2 goodness of fit stat for source prof model	
96	UVISTA_Ks_DRIFT	UVISTA_Ks distance travelled from RA,Dec model centroid	arcsec
97	UVISTA_Ks_VALID	UVISTA_Ks flag=False if FLUX/MAG or its error is not trustworthy	
98	UVISTA_NB118_FLUX	UVISTA_NB118 flux density	uJy
99	UVISTA_NB118_FLUXERR	UVISTA_NB118 flux density error	uJy
100	UVISTA_NB118_MAG	UVISTA_NB118 AB magnitude	mag
101	UVISTA_NB118_MAGERR	UVISTA_NB118 AB magnitude error	mag
102	UVISTA_NB118_CHISQ	UVISTA_NB118 reduced Chi2 goodness of fit stat for source prof model	
103	UVISTA_NB118_DRIFT	UVISTA_NB118 distance travelled from RA,Dec model centroid	arcsec
104	UVISTA_NB118_VALID	UVISTA_NB118 flag=False if FLUX/MAG or its error is not trustworthy	
105	SC_IB427_FLUX	SC_IB427 flux density	uJy
106	SC_IB427_FLUXERR	SC_IB427 flux density error	uJy
107	SC_IB427_MAG	SC_IB427 AB magnitude	mag
108	SC_IB427_MAGERR	SC_IB427 AB magnitude error	mag
109	SC_IB427_CHISQ	SC_IB427 reduced Chi2 goodness of fit stat for source prof model	
110	SC_IB427_DRIFT	SC_IB427 distance travelled from RA,Dec model centroid	arcsec
111	SC_IB427_VALID	SC_IB427 flag=False if FLUX/MAG or its error is not trustworthy	
112	SC_IB464_FLUX	SC_IB464 flux density	uJy
113	SC_IB464_FLUXERR	SC_IB464 flux density error	uJy
114	SC_IB464_MAG	SC_IB464 AB magnitude	mag
115	SC_IB464_MAGERR	SC_IB464 AB magnitude error	mag
116	SC_IB464_CHISQ	SC_IB464 reduced Chi2 goodness of fit stat for source prof model	
117	SC_IB464_DRIFT	SC_IB464 distance travelled from RA,Dec model centroid	arcsec
118	SC_IB464_VALID	SC_IB464 flag=False if FLUX/MAG or its error is not trustworthy	
119	SC_IA484_FLUX	SC_IA484 flux density	uJy
120	SC_IA484_FLUXERR	SC_IA484 flux density error	uJy
121	SC_IA484_MAG	SC_IA484 AB magnitude	mag
122	SC_IA484_MAGERR	SC_IA484 AB magnitude error	mag
123	SC_IA484_CHISQ	SC_IA484 reduced Chi2 goodness of fit stat for source prof model	
124	SC_IA484_DRIFT	SC_IA484 distance travelled from RA,Dec model centroid	arcsec
125	SC_IA484_VALID	SC_IA484 flag=False if FLUX/MAG or its error is not trustworthy	
126	SC_IB505_FLUX	SC_IB505 flux density	uJy
127	SC_IB505_FLUXERR	SC_IB505 flux density error	uJy
128	SC_IB505_MAG	SC_IB505 AB magnitude	mag
129	SC_IB505_MAGERR	SC_IB505 AB magnitude error	mag
130	SC_IB505_CHISQ	SC_IB505 reduced Chi2 goodness of fit stat for source prof model	
131	SC_IB505_DRIFT	SC_IB505 distance travelled from RA,Dec model centroid	arcsec
132	SC_IB505_VALID	SC_IB505 flag=False if FLUX/MAG or its error is not trustworthy	
133	SC_IA527_FLUX	SC_IA527 flux density	uJy
134	SC_IA527_FLUXERR	SC_IA527 flux density error	uJy

135	SC_IA527_MAG	SC_IA527 AB magnitude	mag
136	SC_IA527_MAGERR	SC_IA527 AB magnitude error	mag
137	SC_IA527_CHISQ	SC_IA527 reduced Chi2 goodness of fit stat for source prof model	
138	SC_IA527_DRIFT	SC_IA527 distance travelled from RA,Dec model centroid	arcsec
139	SC_IA527_VALID	SC_IA527 flag=False if FLUX/MAG or its error is not trustworthy	
140	SC_IB574_FLUX	SC_IB574 flux density	uJy
141	SC_IB574_FLUXERR	SC_IB574 flux density error	uJy
142	SC_IB574_MAG	SC_IB574 AB magnitude	mag
143	SC_IB574_MAGERR	SC_IB574 AB magnitude error	mag
144	SC_IB574_CHISQ	SC_IB574 reduced Chi2 goodness of fit stat for source prof model	
145	SC_IB574_DRIFT	SC_IB574 distance travelled from RA,Dec model centroid	arcsec
146	SC_IB574_VALID	SC_IB574 flag=False if FLUX/MAG or its error is not trustworthy	
147	SC_IA624_FLUX	SC_IA624 flux density	uJy
148	SC_IA624_FLUXERR	SC_IA624 flux density error	uJy
149	SC_IA624_MAG	SC_IA624 AB magnitude	mag
150	SC_IA624_MAGERR	SC_IA624 AB magnitude error	mag
151	SC_IA624_CHISQ	SC_IA624 reduced Chi2 goodness of fit stat for source prof model	
152	SC_IA624_DRIFT	SC_IA624 distance travelled from RA,Dec model centroid	arcsec
153	SC_IA624_VALID	SC_IA624 flag=False if FLUX/MAG or its error is not trustworthy	
154	SC_IA679_FLUX	SC_IA679 flux density	uJy
155	SC_IA679_FLUXERR	SC_IA679 flux density error	uJy
156	SC_IA679_MAG	SC_IA679 AB magnitude	mag
157	SC_IA679_MAGERR	SC_IA679 AB magnitude error	mag
158	SC_IA679_CHISQ	SC_IA679 reduced Chi2 goodness of fit stat for source prof model	
159	SC_IA679_DRIFT	SC_IA679 distance travelled from RA,Dec model centroid	arcsec
160	SC_IA679_VALID	SC_IA679 flag=False if FLUX/MAG or its error is not trustworthy	
161	SC_IB709_FLUX	SC_IB709 flux density	uJy
162	SC_IB709_FLUXERR	SC_IB709 flux density error	uJy
163	SC_IB709_MAG	SC_IB709 AB magnitude	mag
164	SC_IB709_MAGERR	SC_IB709 AB magnitude error	mag
165	SC_IB709_CHISQ	SC_IB709 reduced Chi2 goodness of fit stat for source prof model	
166	SC_IB709_DRIFT	SC_IB709 distance travelled from RA,Dec model centroid	arcsec
167	SC_IB709_VALID	SC_IB709 flag=False if FLUX/MAG or its error is not trustworthy	
168	SC_IA738_FLUX	SC_IA738 flux density	uJy
169	SC_IA738_FLUXERR	SC_IA738 flux density error	uJy
170	SC_IA738_MAG	SC_IA738 AB magnitude	mag
171	SC_IA738_MAGERR	SC_IA738 AB magnitude error	mag
172	SC_IA738_CHISQ	SC_IA738 reduced Chi2 goodness of fit stat for source prof model	
173	SC_IA738_DRIFT	SC_IA738 distance travelled from RA,Dec model centroid	arcsec
174	SC_IA738_VALID	SC_IA738 flag=False if FLUX/MAG or its error is not trustworthy	
175	SC_IA767_FLUX	SC_IA767 flux density	uJy
176	SC_IA767_FLUXERR	SC_IA767 flux density error	uJy
177	SC_IA767_MAG	SC_IA767 AB magnitude	mag
178	SC_IA767_MAGERR	SC_IA767 AB magnitude error	mag
179	SC_IA767_CHISQ	SC_IA767 reduced Chi2 goodness of fit stat for source prof model	
180	SC_IA767_DRIFT	SC_IA767 distance travelled from RA,Dec model centroid	arcsec
181	SC_IA767_VALID	SC_IA767 flag=False if FLUX/MAG or its error is not trustworthy	
182	SC_IB827_FLUX	SC_IB827 flux density	uJy
183	SC_IB827_FLUXERR	SC_IB827 flux density error	uJy
184	SC_IB827_MAG	SC_IB827 AB magnitude	mag
185	SC_IB827_MAGERR	SC_IB827 AB magnitude error	mag
186	SC_IB827_CHISQ	SC_IB827 reduced Chi2 goodness of fit stat for source prof model	
187	SC_IB827_DRIFT	SC_IB827 distance travelled from RA,Dec model centroid	arcsec
188	SC_IB827_VALID	SC_IB827 flag=False if FLUX/MAG or its error is not trustworthy	
189	SC_NB711_FLUX	SC_NB711 flux density	uJy
190	SC_NB711_FLUXERR	SC_NB711 flux density error	uJy
191	SC_NB711_MAG	SC_NB711 AB magnitude	mag
192	SC_NB711_MAGERR	SC_NB711 AB magnitude error	mag
193	SC_NB711_CHISQ	SC_NB711 reduced Chi2 goodness of fit stat for source prof model	
194	SC_NB711_DRIFT	SC_NB711 distance travelled from RA,Dec model centroid	arcsec
195	SC_NB711_VALID	SC_NB711 flag=False if FLUX/MAG or its error is not trustworthy	
196	SC_NB816_FLUX	SC_NB816 flux density	uJy
197	SC_NB816_FLUXERR	SC_NB816 flux density error	uJy
198	SC_NB816_MAG	SC_NB816 AB magnitude	mag
199	SC_NB816_MAGERR	SC_NB816 AB magnitude error	mag

```
200 | SC_NB816_CHISQ       | SC_NB816 reduced Chi2 goodness of fit stat for source prof model     |
201 | SC_NB816_DRIFT       | SC_NB816 distance travelled from RA,Dec model centroid               | arcsec
202 | SC_NB816_VALID       | SC_NB816 flag=False if FLUX/MAG or its error is not trustworthy      |
203 | IRAC_CH1_FLUX        | IRAC_CH1 flux density                                                | uJy
204 | IRAC_CH1_FLUXERR     | IRAC_CH1 flux density error                                          | uJy
205 | IRAC_CH1_MAG         | IRAC_CH1 AB magnitude                                                | mag
206 | IRAC_CH1_MAGERR      | IRAC_CH1 AB magnitude error                                          | mag
207 | IRAC_CH1_CHISQ       | IRAC_CH1 reduced Chi2 goodness of fit stat for source prof model     |
208 | IRAC_CH1_DRIFT       | IRAC_CH1 distance travelled from RA,Dec model centroid               | arcsec
209 | IRAC_CH1_VALID       | IRAC_CH1 flag=False if FLUX/MAG or its error is not trustworthy      |
210 | IRAC_CH2_FLUX        | IRAC_CH2 flux density                                                | uJy
211 | IRAC_CH2_FLUXERR     | IRAC_CH2 flux density error                                          | uJy
212 | IRAC_CH2_MAG         | IRAC_CH2 AB magnitude                                                | mag
213 | IRAC_CH2_MAGERR      | IRAC_CH2 AB magnitude error                                          | mag
214 | IRAC_CH2_CHISQ       | IRAC_CH2 reduced Chi2 goodness of fit stat for source prof model     |
215 | IRAC_CH2_DRIFT       | IRAC_CH2 distance travelled from RA,Dec model centroid               | arcsec
216 | IRAC_CH2_VALID       | IRAC_CH2 flag=False if FLUX/MAG or its error is not trustworthy      |
217 | IRAC_CH3_FLUX        | IRAC_CH3 flux density                                                | uJy
218 | IRAC_CH3_FLUXERR     | IRAC_CH3 flux density error                                          | uJy
219 | IRAC_CH3_MAG         | IRAC_CH3 AB magnitude                                                | mag
220 | IRAC_CH3_MAGERR      | IRAC_CH3 AB magnitude error                                          | mag
221 | IRAC_CH3_CHISQ       | IRAC_CH3 reduced Chi2 goodness of fit stat for source prof model     |
222 | IRAC_CH3_DRIFT       | IRAC_CH3 distance travelled from RA,Dec model centroid               | arcsec
223 | IRAC_CH3_VALID       | IRAC_CH3 flag=False if FLUX/MAG or its error is not trustworthy      |
224 | IRAC_CH4_FLUX        | IRAC_CH4 flux density                                                | uJy
225 | IRAC_CH4_FLUXERR     | IRAC_CH4 flux density error                                          | uJy
226 | IRAC_CH4_MAG         | IRAC_CH4 AB magnitude                                                | mag
227 | IRAC_CH4_MAGERR      | IRAC_CH4 AB magnitude error                                          | mag
228 | IRAC_CH4_CHISQ       | IRAC_CH4 reduced Chi2 goodness of fit stat for source prof model     |
229 | IRAC_CH4_DRIFT       | IRAC_CH4 distance travelled from RA,Dec model centroid               | arcsec
230 | IRAC_CH4_VALID       | IRAC_CH4 flag=False if FLUX/MAG or its error is not trustworthy      |
231 | ID_GALEX             | ID in GALEX cat. (Zamojski+2007, Capak+2007), crossm. with 0.6" rad. |
232 | GALEX_NUV_FLUX       | GALEX_NUV flux density                                               | uJy
233 | GALEX_NUV_FLUXERR    | GALEX_NUV flux density error                                         | uJy
234 | GALEX_NUV_MAG        | GALEX_NUV AB magnitude                                               | mag
235 | GALEX_NUV_MAGERR     | GALEX_NUV AB magnitude error                                         | mag
236 | GALEX_FUV_FLUX       | GALEX_FUV flux density                                               | uJy
237 | GALEX_FUV_FLUXERR    | GALEX_FUV flux density error                                         | uJy
238 | GALEX_FUV_MAG        | GALEX_FUV AB magnitude                                               | mag
239 | GALEX_FUV_MAGERR     | GALEX_FUV AB magnitude error                                         | mag
240 | ID_COSMOS2015        | ID in COSMOS2015 cat. (Laigle+2016), crossmatched with 0.6" radius   |
241 | SPLASH_CH1_FLUX      | SPLASH_CH1 flux density                                              | uJy
242 | SPLASH_CH1_FLUXERR   | SPLASH_CH1 flux density error                                        | uJy
243 | SPLASH_CH1_MAG       | SPLASH_CH1 AB magnitude                                              | mag
244 | SPLASH_CH1_MAGERR    | SPLASH_CH1 AB magnitude error                                        | mag
245 | SPLASH_CH2_FLUX      | SPLASH_CH2 flux density                                              | uJy
246 | SPLASH_CH2_FLUXERR   | SPLASH_CH2 flux density error                                        | uJy
247 | SPLASH_CH2_MAG       | SPLASH_CH2 AB magnitude                                              | mag
248 | SPLASH_CH2_MAGERR    | SPLASH_CH2 AB magnitude error                                        | mag
249 | SPLASH_CH3_FLUX      | SPLASH_CH3 flux density                                              | uJy
250 | SPLASH_CH3_FLUXERR   | SPLASH_CH3 flux density error                                        | uJy
251 | SPLASH_CH3_MAG       | SPLASH_CH3 AB magnitude                                              | mag
252 | SPLASH_CH3_MAGERR    | SPLASH_CH3 AB magnitude error                                        | mag
253 | SPLASH_CH4_FLUX      | SPLASH_CH4 flux density                                              | uJy
254 | SPLASH_CH4_FLUXERR   | SPLASH_CH4 flux density error                                        | uJy
255 | SPLASH_CH4_MAG       | SPLASH_CH4 AB magnitude                                              | mag
256 | SPLASH_CH4_MAGERR    | SPLASH_CH4 AB magnitude error                                        | mag
257 | ID_ACS               | ID in HST ACS F814W cat. (Leauthaud+2007), crossm. with 0.6" radius  |
258 | ACS_F814W_MAG        | ACS_F814W AB magnitude                                               | mag
259 | ACS_F814W_MAGERR     | ACS_F814W AB magnitude error                                         | mag
260 | ACS_F814W_FLUX       | ACS_F814W flux density                                               | uJy
261 | ACS_F814W_FLUXERR    | ACS_F814W flux density error                                         | uJy
262 | ACS_A_WORLD          | ACS F814W semi-major axis length                                     | deg
263 | ACS_B_WORLD          | ACS F814W semi-minor axis length                                     | deg
264 | ACS_THETA_WORLD      | ACS F814W angle; to get PA measured from N through E, add/subtr. 90  | deg
```

265	ACS_FWHM_WORLD	ACS F814W FWHM assuming a gaussian core	deg
266	ACS_MU_MAX	ACS F814W peak surface brightness above background	
267	ACS_MU_CLASS	ACS F814W star/galaxy classifier: 1=galaxy, 2=star, 3=fake detection	
268	ID_CHANDRA	ID in Chandra cat. (Civano+2016, Marchesi+2016), crossm. w. 0.6" rad	
269	ID_CLASSIC	ID in the Classic catalogue, crossmatched with 0.6" radius	
270	lp_zBEST	LePhare photo-z (=lp_zPDF if galaxy, NaN if X-ray source or masked)	
271	lp_type	LePhare type (0: galaxy, 1: star, 2: Xray sour., -9: failure in fit)	
272	lp_zPDF	LePhare photo-z using the galaxy templ., median of likelihood distr.	
273	lp_zPDF_l68	LePhare photo-z lower limit, 68% confidence level (galaxy templates)	
274	lp_zPDF_u68	LePhare photo-z upper limit, 68% confidence level (galaxy templates)	
275	lp_zMinChi2	LePhare photo-z using the galaxy templates, minimum chi2	
276	lp_chi2_best	LePhare reduced chi2 for lp_zMinChi2 (NaN if less than 3 filters)	
277	lp_zp_2	LePhare 2nd photo-z solution if a 2nd peak detected w. P>5% in PDF	
278	lp_chi2_2	LePhare reduced chi2 for the second photo-z solution	
279	lp_NbFilt	LePhare number of filters used in the fit	
280	lp_zq	LePhare photo-z for the AGN library	
281	lp_chiq	LePhare reduced chi2 for photo-z for the AGN library	
282	lp_modq	LePhare best fit template number in the AGN library	
283	lp_mods	LePhare best fit template number in the star library	
284	lp_chis	LePhare reduced chi2 for the best fit with the star library	
285	lp_mask	LePhare mask flag (0: in UVISTA and in clean part of HSC and SUPCAM)	
286	lp_model	LePhare BC03 best fit template number	
287	lp_age	LePhare BC03 age of best fit template at zPDF	yr
288	lp_dust	LePhare BC03 colour excess E(B-V) of best fit template at zPDF	
289	lp_Attenuation	LePhare BC03 best-fit dust law number at zPDF	
290	lp_MFUV	LePhare BC03 absolute rest-frame AB mag in GALEX FUV band at zPDF	mag
291	lp_MNUV	LePhare BC03 absolute rest-frame AB mag in GALEX NUV band at zPDF	mag
292	lp_MU	LePhare BC03 absolute rest-frame AB mag in CFHT u* band at zPDF	mag
293	lp_MG	LePhare BC03 absolute rest-frame AB mag in Subaru/HSC g band at zPDF	mag
294	lp_MR	LePhare BC03 absolute rest-frame AB mag in Subaru/HSC r band at zPDF	mag
295	lp_MI	LePhare BC03 absolute rest-frame AB mag in Subaru/HSC i band at zPDF	mag
296	lp_MZ	LePhare BC03 absolute rest-frame AB mag in Subaru/HSC z band at zPDF	mag
297	lp_MY	LePhare BC03 absolute rest-frame AB mag in VISTA Y band at zPDF	mag
298	lp_MJ	LePhare BC03 absolute rest-frame AB mag in VISTA J band at zPDF	mag
299	lp_MH	LePhare BC03 absolute rest-frame AB mag in VISTA H band at zPDF	mag
300	lp_MK	LePhare BC03 absolute rest-frame AB mag in VISTA Ks band at zPDF	mag
301	lp_mass_med	LePhare BC03 log stellar mass at zPDF	log(solMass)
302	lp_mass_med_min68	LePhare BC03 log stellar mass at zPDF, lower limit, 68% conf. level	log(solMass)
303	lp_mass_med_max68	LePhare BC03 log stellar mass at zPDF, upper limit, 68% conf. level	log(solMass)
304	lp_mass_best	LePhare BC03 log stellar mass at zMinChi2	log(solMass)
305	lp_SFR_med	LePhare BC03 log SFR at zPDF	log(solMass/yr)
306	lp_SFR_med_min68	LePhare BC03 log SFR at zPDF, lower limit, 68% confidence level	log(solMass/yr)
307	lp_SFR_med_max68	LePhare BC03 log SFR at zPDF, upper limit, 68% confidence level	log(solMass/yr)
308	lp_SFR_best	LePhare BC03 log SFR at zMinChi2	log(solMass/yr)
309	lp_sSFR_med	LePhare BC03 log sSFR at zPDF	log(yr**(-1))
310	lp_sSFR_med_min68	LePhare BC03 log sSFR at zPDF, lower limit, 68% confidence level	log(yr**(-1))
311	lp_sSFR_med_max68	LePhare BC03 log sSFR at zPDF, upper limit, 68% confidence level	log(yr**(-1))
312	lp_sSFR_best	LePhare BC03 log sSFR at zMinChi2	log(yr**(-1))
313	ez_z_phot	EAZY maximum a-posteriori photo-z	
314	ez_z_phot_chi2	EAZY chi2 at ez_z_phot, with z-prior	
315	ez_z_phot_risk	EAZY risk parameter (Tanaka+2018) at ez_z_phot, R(ez_z_phot)	
316	ez_z_min_risk	EAZY photo-z where risk parameter R(z) is minimised	
317	ez_min_risk	EAZY risk parameter at ez_z_min_risk, R(ez_z_min_risk)	
318	ez_z_raw_chi2	EAZY photo-z where chi2 is minimised, without priors	
319	ez_raw_chi2	EAZY chi2 at ez_z_raw_chi2	
320	ez_z025	EAZY 2.5% percentile of photo-z	
321	ez_z160	EAZY 16.0% percentile of photo-z	
322	ez_z500	EAZY 50.0% percentile of photo-z	
323	ez_z840	EAZY 84.0% percentile of photo-z	
324	ez_z975	EAZY 97.5% percentile of photo-z	
325	ez_nusefilt	EAZY no. of filters used for photo-z (only filters w/o missing data)	
326	ez_lc_min	EAZY minimum effective wavelength of valid filters	Angstrom
327	ez_lc_max	EAZY minimum effective wavelength of valid filters	Angstrom
328	ez_star_min_chi2	EAZY chi2 best stellar template fit (BT-SETTL models) as, 8% sys unc	
329	ez_star_teff	EAZY effective temperature of the stellar template	K

330	ez_restU	EAZY rest-frame U-band flux density	uJy
331	ez_restU_err	EAZY rest-frame U-band flux density uncertainty	uJy
332	ez_restB	EAZY rest-frame B-band flux density	uJy
333	ez_restB_err	EAZY rest-frame B-band flux density uncertainty	uJy
334	ez_restV	EAZY rest-frame V-band flux density	uJy
335	ez_restV_err	EAZY rest-frame V-band flux density uncertainty	uJy
336	ez_restJ	EAZY rest-frame J-band flux density	uJy
337	ez_restJ_err	EAZY rest-frame J-band flux density uncertainty	uJy
338	ez_dL	EAZY luminosity distance at ez_z_phot	Mpc
339	ez_mass	EAZY log stellar mass	log(solMass)
340	ez_sfr	EAZY log SFR	log(solMass/yr)
341	ez_ssfr	EAZY log sSFR	log(yr**(-1))
342	ez_Lv	EAZY log V-band luminosity	log(solLum)
343	ez_LIR	EAZY total 8-1000 um luminosity	solLum
344	ez_energy_abs	EAZY implied absorbed energy associated with Av	solLum
345	ez_Lu	EAZY luminosity in rest-frame U band	solLum
346	ez_Lj	EAZY luminosity in rest-frame J band	solLum
347	ez_L1400	EAZY luminosity in tophat filter at 1400 A (200 A wide) rest-frame	solLum
348	ez_L2800	EAZY luminosity in tophat filter at 2800 A (200 A wide) rest-frame	solLum
349	ez_LHa	EAZY Halpha line luminosity (reddened)	solLum
350	ez_LOIII	EAZY [OIII] 4959+5007 line luminosity (reddened)	solLum
351	ez_LHb	EAZY Hbeta line luminosity (reddened)	solLum
352	ez_LOII	EAZY [OII] 3726+3729 line luminosity (reddened)	solLum
353	ez_MLv	EAZY mass-to-light ratio in V band	solMass/solLum
354	ez_Av	EAZY extinction in V band	mag
355	ez_lwAgeV	EAZY light-weighted age in the V band	Gyr
356	ez_mass_p025	EAZY 2.5% percentile of log stellar mass	log(solMass)
357	ez_mass_p160	EAZY 16.0% percentile of log stellar mass	log(solMass)
358	ez_mass_p500	EAZY 50.0% percentile of log stellar mass	log(solMass)
359	ez_mass_p840	EAZY 84.0% percentile of log stellar mass	log(solMass)
360	ez_mass_p975	EAZY 97.5% percentile of log stellar mass	log(solMass)
361	ez_sfr_p025	EAZY 2.5% percentile of log SFR	log(solMass/yr)
362	ez_sfr_p160	EAZY 16.0% percentile of log SFR	log(solMass/yr)
363	ez_sfr_p500	EAZY 50.0% percentile of log SFR	log(solMass/yr)
364	ez_sfr_p840	EAZY 84.0% percentile of log SFR	log(solMass/yr)
365	ez_sfr_p975	EAZY 97.5% percentile of log SFR	log(solMass/yr)
366	ez_Lv_p025	EAZY 2.5% percentile of log V-band luminosity	log(solLum)
367	ez_Lv_p160	EAZY 16.0% percentile of log V-band luminosity	log(solLum)
368	ez_Lv_p500	EAZY 50.0% percentile of log V-band luminosity	log(solLum)
369	ez_Lv_p840	EAZY 84.0% percentile of log V-band luminosity	log(solLum)
370	ez_Lv_p975	EAZY 97.5% percentile of log V-band luminosity	log(solLum)
371	ez_LIR_p025	EAZY 2.5% percentile of total 8-1000 um luminosity	solLum
372	ez_LIR_p160	EAZY 16.0% percentile of total 8-1000 um luminosity	solLum
373	ez_LIR_p500	EAZY 50.0% percentile of total 8-1000 um luminosity	solLum
374	ez_LIR_p840	EAZY 84.0% percentile of total 8-1000 um luminosity	solLum
375	ez_LIR_p975	EAZY 97.5% percentile of total 8-1000 um luminosity	solLum
376	ez_energy_abs_p025	EAZY 2.5% percentile of implied absorbed energy associated with Av	solLum
377	ez_energy_abs_p160	EAZY 16.0% percentile of implied absorbed energy associated with Av	solLum
378	ez_energy_abs_p500	EAZY 50.0% percentile of implied absorbed energy associated with Av	solLum
379	ez_energy_abs_p840	EAZY 84.0% percentile of implied absorbed energy associated with Av	solLum
380	ez_energy_abs_p975	EAZY 97.5% percentile of implied absorbed energy associated with Av	solLum
381	ez_Lu_p025	EAZY 2.5% percentile of luminosity in rest-frame U band	solLum
382	ez_Lu_p160	EAZY 16.0% percentile of luminosity in rest-frame U band	solLum
383	ez_Lu_p500	EAZY 50.0% percentile of luminosity in rest-frame U band	solLum
384	ez_Lu_p840	EAZY 84.0% percentile of luminosity in rest-frame U band	solLum
385	ez_Lu_p975	EAZY 97.5% percentile of luminosity in rest-frame U band	solLum
386	ez_Lj_p025	EAZY 2.5% percentile of luminosity in rest-frame J band	solLum
387	ez_Lj_p160	EAZY 16.0% percentile of luminosity in rest-frame J band	solLum
388	ez_Lj_p500	EAZY 50.0% percentile of luminosity in rest-frame J band	solLum
389	ez_Lj_p840	EAZY 84.0% percentile of luminosity in rest-frame J band	solLum
390	ez_Lj_p975	EAZY 97.5% percentile of luminosity in rest-frame J band	solLum
391	ez_L1400_p025	EAZY 2.5% percentile of lum tophat filter at 1400 A (200 A wide) rf	solLum
392	ez_L1400_p160	EAZY 16.0% percentile of lum tophat filter at 1400 A (200 A wide) rf	solLum
393	ez_L1400_p500	EAZY 50.0% percentile of lum tophat filter at 1400 A (200 A wide) rf	solLum
394	ez_L1400_p840	EAZY 84.0% percentile of lum tophat filter at 1400 A (200 A wide) rf	solLum

395	ez_L1400_p975	EAZY 97.5% percentile of lum tophat filter at 1400 A (200 A wide) rf	solLum
396	ez_L2800_p025	EAZY 2.5% percentile of lum tophat filter at 2800 A (200 A wide) rf	solLum
397	ez_L2800_p160	EAZY 16.0% percentile of lum tophat filter at 2800 A (200 A wide) rf	solLum
398	ez_L2800_p500	EAZY 50.0% percentile of lum tophat filter at 2800 A (200 A wide) rf	solLum
399	ez_L2800_p840	EAZY 84.0% percentile of lum tophat filter at 2800 A (200 A wide) rf	solLum
400	ez_L2800_p975	EAZY 97.5% percentile of lum tophat filter at 2800 A (200 A wide) rf	solLum
401	ez_LHa_p025	EAZY 2.5% percentile of Halpha line luminosity (reddened)	solLum
402	ez_LHa_p160	EAZY 16.0% percentile of Halpha line luminosity (reddened)	solLum
403	ez_LHa_p500	EAZY 50.0% percentile of Halpha line luminosity (reddened)	solLum
404	ez_LHa_p840	EAZY 84.0% percentile of Halpha line luminosity (reddened)	solLum
405	ez_LHa_p975	EAZY 97.5% percentile of Halpha line luminosity (reddened)	solLum
406	ez_LOIII_p025	EAZY 2.5% percentile of [OIII] 4959+5007 line luminosity (reddened)	solLum
407	ez_LOIII_p160	EAZY 16.0% percentile of [OIII] 4959+5007 line luminosity (reddened)	solLum
408	ez_LOIII_p500	EAZY 50.0% percentile of [OIII] 4959+5007 line luminosity (reddened)	solLum
409	ez_LOIII_p840	EAZY 84.0% percentile of [OIII] 4959+5007 line luminosity (reddened)	solLum
410	ez_LOIII_p975	EAZY 97.5% percentile of [OIII] 4959+5007 line luminosity (reddened)	solLum
411	ez_LHb_p025	EAZY 2.5% percentile of Hbeta line luminosity (reddened)	solLum
412	ez_LHb_p160	EAZY 16.0% percentile of Hbeta line luminosity (reddened)	solLum
413	ez_LHb_p500	EAZY 50.0% percentile of Hbeta line luminosity (reddened)	solLum
414	ez_LHb_p840	EAZY 84.0% percentile of Hbeta line luminosity (reddened)	solLum
415	ez_LHb_p975	EAZY 97.5% percentile of Hbeta line luminosity (reddened)	solLum
416	ez_LOII_p025	EAZY 2.5% percentile of [OII] 3726+3729 line luminosity (reddened)	solLum
417	ez_LOII_p160	EAZY 16.0% percentile of [OII] 3726+3729 line luminosity (reddened)	solLum
418	ez_LOII_p500	EAZY 50.0% percentile of [OII] 3726+3729 line luminosity (reddened)	solLum
419	ez_LOII_p840	EAZY 84.0% percentile of [OII] 3726+3729 line luminosity (reddened)	solLum
420	ez_LOII_p975	EAZY 97.5% percentile of [OII] 3726+3729 line luminosity (reddened)	solLum
421	ez_ssfr_p025	EAZY 2.5% percentile of log sSFR	log(yr**(-1))
422	ez_ssfr_p160	EAZY 16.0% percentile of log sSFR	log(yr**(-1))
423	ez_ssfr_p500	EAZY 50.0% percentile of log sSFR	log(yr**(-1))
424	ez_ssfr_p840	EAZY 84.0% percentile of log sSFR	log(yr**(-1))
425	ez_ssfr_p975	EAZY 97.5% percentile of log sSFR	log(yr**(-1))
426	ez_Av_p025	EAZY 2.5% percentile of extinction in V band	mag
427	ez_Av_p160	EAZY 16.0% percentile of extinction in V band	mag
428	ez_Av_p500	EAZY 50.0% percentile of extinction in V band	mag
429	ez_Av_p840	EAZY 84.0% percentile of extinction in V band	mag
430	ez_Av_p975	EAZY 97.5% percentile of extinction in V band	mag

References

Arnouts, S., Moscardini, L., Vanzella, E., et al. 2002, MNRAS, 329, 355

Astropy Collaboration, Price-Whelan, A. M., Sipőcz, B. M., et al. 2018, The Astronomical Journal, 156, 123, aDS Bibcode: 2018AJ....156..123A

Barbary, K. 2016, The Journal of Open Source Software, 1, 58

Bertin, E. & Arnouts, S. 1996, A&AS, 117, 393

Brammer, G. B., van Dokkum, P. G., & Coppi, P. 2008, ApJ, 686, 1503

Drlica-Wagner, A., Sevilla-Noarbe, I., Rykoff, E. S., et al. 2018, ApJS, 235, 33

Gaia Collaboration, Brown, A. G. A., Vallenari, A., et al. 2016, Astronomy & Astrophysics, 595, A2

Gaia Collaboration, Brown, A. G. A., Vallenari, A., et al. 2018, Astronomy & Astrophysics, 616, A1

Hsieh, B.-C., Wang, W.-H., Hsieh, C.-C., et al. 2012, The Astrophysical Journal Supplement Series, 203, 23

Ilbert, O., Arnouts, S., McCracken, H. J., et al. 2006, A&A, 457, 841

Laigle, C., McCracken, H. J., Ilbert, O., et al. 2016, ApJS, 224, 24

Lang, D., Hogg, D. W., & Mykytyn, D. 2016, Astrophysics Source Code Library, ascl:1604.008

McCracken, H. J., Milvang-Jensen, B., Dunlop, J., et al. 2012, Astronomy and Astrophysics, 544, A156

Robitaille, T. P., Tollerud, E. J., Greenfield, P., et al. 2013, Astronomy & Astrophysics, 558, A33, publisher: EDP Sciences

Taylor, M. B. 2006, in Astronomical Society of the Pacific Conference Series, Vol. 351, Astronomical Data Analysis Software and Systems XV, ed. C. Gabriel, C. Arviset, D. Ponz, & S. Enrique, 666

Weaver, J. R., Kauffmann, O. B., Ilbert, O., et al. 2022, ApJS, 258, 11